



**HAL**  
open science

## III-Nitride-on-silicon microdisk lasers from the blue to the deep ultra-violet

Julien Selles, V. Crepel, I. Roland, M. El Kurdi, X. Checoury, P. Boucaud, Meletios Mexis, M. Leroux, B. Damilano, S. Rennesson, et al.

► **To cite this version:**

Julien Selles, V. Crepel, I. Roland, M. El Kurdi, X. Checoury, et al.. III-Nitride-on-silicon microdisk lasers from the blue to the deep ultra-violet. *Applied Physics Letters*, 2016, 109 (23), pp.231101. 10.1063/1.4971357 . hal-01469387

**HAL Id: hal-01469387**

**<https://hal.science/hal-01469387>**

Submitted on 3 Jun 2021

**HAL** is a multi-disciplinary open access archive for the deposit and dissemination of scientific research documents, whether they are published or not. The documents may come from teaching and research institutions in France or abroad, or from public or private research centers.

L'archive ouverte pluridisciplinaire **HAL**, est destinée au dépôt et à la diffusion de documents scientifiques de niveau recherche, publiés ou non, émanant des établissements d'enseignement et de recherche français ou étrangers, des laboratoires publics ou privés.

### III-Nitride-on-silicon microdisk lasers from the blue to the deep ultra-violet

J. Sellés, V. Crepel, I. Roland, M. El Kurdi, X. Checoury, P. Boucaud, M. Mexis, M. Leroux, B. Damilano, S. Rennesson, F. Semond, B. Gayral, C. Brimont, and T. Guillet

Citation: [Applied Physics Letters](#) **109**, 231101 (2016); doi: 10.1063/1.4971357

View online: <http://dx.doi.org/10.1063/1.4971357>

View Table of Contents: <http://scitation.aip.org/content/aip/journal/apl/109/23?ver=pdfcov>

Published by the [AIP Publishing](#)

---

#### Articles you may be interested in

[Lasing properties of non-polar GaN quantum dots in cubic aluminum nitride microdisk cavities](#)

*Appl. Phys. Lett.* **103**, 021107 (2013); 10.1063/1.4813408

[High quality nitride based microdisks obtained via selective wet etching of AlInN sacrificial layers](#)

*Appl. Phys. Lett.* **92**, 171102 (2008); 10.1063/1.2917452

[Visible submicron microdisk lasers](#)

*Appl. Phys. Lett.* **90**, 111119 (2007); 10.1063/1.2714312

[Blue lasing at room temperature in high quality factor Ga N/Al In N microdisks with InGaN quantum wells](#)

*Appl. Phys. Lett.* **90**, 061106 (2007); 10.1063/1.2460234

[Optical modes within III-nitride multiple quantum well microdisk cavities](#)

*Appl. Phys. Lett.* **72**, 1530 (1998); 10.1063/1.120573

---

The advertisement features the Lake Shore CRYOTRONICS logo on the left, which includes a blue square icon with a white 'L' and the text 'Lake Shore CRYOTRONICS'. In the center is a photograph of a large, industrial-grade cryogenic measurement system with a computer monitor and various sensors. On the right, the text reads 'NEW 8600 Series VSM' in large orange letters, followed by 'For fast, highly sensitive measurement performance' in white. At the bottom right, there is a 'LEARN MORE' button with a right-pointing arrow.

### III-Nitride-on-silicon microdisk lasers from the blue to the deep ultra-violet

J. Sellés,<sup>1</sup> V. Crepel,<sup>1</sup> I. Roland,<sup>2</sup> M. El Kurdi,<sup>2</sup> X. Checoury,<sup>2</sup> P. Boucaud,<sup>2</sup> M. Mexis,<sup>3</sup> M. Leroux,<sup>3</sup> B. Damilano,<sup>3</sup> S. Rennesson,<sup>3</sup> F. Semond,<sup>3</sup> B. Gayral,<sup>4,5</sup> C. Brimont,<sup>1</sup> and T. Guillet<sup>1,a)</sup>

<sup>1</sup>Laboratoire Charles Coulomb (L2C), UMR 5221 CNRS-Université de Montpellier, F-34095 Montpellier, France

<sup>2</sup>Centre de Nanosciences et de Nanotechnologies, CNRS, Univ. Paris-Sud, Université Paris-Saclay, Bâtiment 220, F-91045 Orsay, France

<sup>3</sup>Centre de Recherche pour l'Hetero-Epitaxie et ses Applications (CRHEA)-CNRS, Rue Bernard Gregory, F-06560 Valbonne, France

<sup>4</sup>Université Grenoble Alpes, F-38000 Grenoble, France

<sup>5</sup>CEA, INAC-PHELIQS, Nanophysique et Semiconducteurs Group, F-38000 Grenoble, France

(Received 19 September 2016; accepted 20 November 2016; published online 5 December 2016)

We present a series of microdisk lasers realized within the same GaN-on-Si photonic platform scheme, and operating at room temperature under pulsed optical pumping over a broad spectral range extending over  $\lambda = 275\text{ nm} - 470\text{ nm}$ . The III-nitride microdisks embed either binary GaN/AlN multiple quantum wells (MQWs) for UV operation, or ternary InGaN/GaN MQWs for violet and blue operation. This demonstrates the versatility of this nitride-on-silicon platform, and the realization on this platform of efficient active layers for lasing action over a 200 nm broad UV to visible spectral range. We probe the lasing threshold carrier density over the whole spectral range and found that it is similar whatever the emission wavelength for these  $Q > 1000$  microdisk resonators with a constant material quality until quantum confined Stark effect takes over. The threshold is also found independent of microdisk diameters from 3 to 12  $\mu\text{m}$ , with a  $\beta$  factor intermediate between the one of vertical cavity lasers and the one of small modal volume “thresholdless” lasers. Published by AIP Publishing. [<http://dx.doi.org/10.1063/1.4971357>]

The integrated photonic platforms are reaching maturity at telecommunication wavelengths, based on Si, GaAs, or (In,Ga)P photonic circuits, emitters, and amplifiers. The development of a similar platform dedicated to the UV and visible spectral range presents a strong interest for biochemical detection applications and on-chip optical interconnects.<sup>1,2</sup> This relies on the realization of efficient and compact microlaser sources that can be coupled to optical waveguides and are compatible with photonic circuitry.<sup>3</sup> Light-emitting diodes (LEDs) and micro-LEDs based on nitride materials, operating in this spectral range, have been developed over the past decade, but the demonstration of microlasers is much more challenging: it imposes stronger requirements on the room-temperature radiative efficiency and on the gain of the active layers. The recent demonstrations of blue and UV microlasers are based either on bulk active layers (GaN or ZnO, at a fixed wavelength  $\lambda = 360$  or  $380\text{ nm}$ )<sup>4-7</sup> or on quantum wells (QWs) and quantum dots (QDs); InGaN QWs,<sup>8-11</sup> fractional QWs,<sup>12</sup> and QDs<sup>13,14</sup> allow for an emission at longer wavelength, from the violet to the blue and even the green<sup>15</sup> in microlasers. Reaching a shorter wavelength requires the use of AlGaIn/AlN quantum wells that are subject to a strong quantum confined Stark effect (QCSE) detrimental to the achievement of gain. A recent demonstration of lasing based on cubic GaN quantum wells is a first attempt to circumvent this difficulty.<sup>16</sup> We can notice that most microlaser demonstrations are based on microdisk resonators that support a large set of whispering

gallery modes (WGMs) whatever the gain spectral range of the emitter; this has paved the way to the more recent realization of lasers based on photonic crystal monomode cavities,<sup>11,12</sup> for which the cavity mode has to be carefully tuned to the gain spectrum of the quantum wells.

Following our recent demonstration of an optically pumped microdisk laser operating at room temperature in the UV-C spectral range, at  $\lambda = 275\text{ nm}$ ,<sup>17</sup> we report in the present letter the realization of a whole series of microdisk lasers based on GaN/AlN and InGaIn/GaN quantum wells, whose emission can be tuned from 275 nm to 470 nm. The deep-UV emission is obtained with ultra-thin binary GaN/AlN quantum wells that are presently investigated as interesting alternatives to AlGaIn/AlN heterostructures.<sup>18</sup> All the microlasers rely on the same nitride-on-silicon platform: the quantum wells are integrated on top of a buffer layer grown on silicon that can be released into a membrane by the selective under-etching of the silicon substrate. The good radiative efficiency of the MBE (molecular beam epitaxy)-grown quantum wells results from the careful control of the crystalline quality of the very thin underlying AlN buffer layer deposited on the Si substrate. The microlasers operate under pulsed optical excitation, and the lasing threshold is reduced by a factor 10 from deep-UV GaN/AlN microdisks to the violet InGaIn/GaN ones. We demonstrate here the broad spectral tunability of this nitride-on-silicon platform (200 nm, i.e., almost an octave) that allows foreseeing a variety of integrated photonics applications, including the multi-color integrated laser sources. All microdisks present Q factors exceeding 1000, for a broad range of geometrical parameters, so that we are able to compare the gain thresholds of the different active layers.

<sup>a)</sup>E-mail: thierry.guillet@umontpellier.fr

TABLE I. Investigated samples, active layers, microdisk geometries, and microlaser characteristics.

Sample	Materials		Quantum wells			Resonator			Laser	
	Well	Barrier	Thickness (nm)	Number	CW wavelength (nm)	Diameter ( $\mu\text{m}$ )	Thickness (nm)	Q	Threshold ( $\text{mJ}\cdot\text{cm}^{-2}$ per pulse)	Wavelength (nm)
GaN-1	GaN	AlN	0.7	20	280	3	220	4000	15	275
GaN-2	GaN	AlN	0.7	10	290	6	160	2000	27	290
GaN-3	GaN	AlN	1.2	10	330	6	160	2000	35	330
GaN-4	GaN	AlN	1.8	10	350	6	160	>1000		
InGaN-1	$\text{In}_{0.12}\text{Ga}_{0.88}\text{N}$	GaN	2.2	10	417	4	515	2500	3	412
InGaN-2	$\text{In}_{0.2}\text{Ga}_{0.8}\text{N}$	GaN	2.2	10	500	5	1300	2500	3	470

Two series of samples are grown by  $\text{NH}_3$ -MBE on Si(111) substrates. The first series, named GaN-x, is ultra-thin GaN/AlN layers. Indeed, the structure consists of a 100 nm AlN buffer layer grown at 1030 °C, followed by 10 or 20 pairs of GaN/AlN multiple quantum wells (MQWs). From a sample to another, the GaN quantum well thickness varies from 0.7 to 1.8 nm whereas the AlN barrier thickness is kept constant at 5 nm. The second series, named InGaN-x, consists of a high crystalline quality AlN buffer layer, followed by a GaN buffer layer. These samples are finished by 10 pairs of 2.2 nm-thick InGaN/9 nm-thick GaN MQWs with two different In content (12% and 20%). The GaN buffer layer is non-intentionally doped in the sample InGaN-1, and Si-doped in the sample InGaN-2 in order to anticipate the electrical injection. The precise description of the active layers is provided in the Table I. The threading dislocation density is of the order of  $10^{10}\text{ cm}^{-2}$ , quite low for thin nitride-on-Si, thanks to the high growth temperature chosen for the AlN buffer layer. The microdisks are then patterned

through electron beam lithography and dry etching techniques. Finally, the high quality AlN/GaN membranes are released through a very selective etching of Si.<sup>19</sup> The same process is used to produce photonic crystal cavities from the UV to the IR spectral range,<sup>20–23</sup> with strong optical nonlinearities in the IR.<sup>24,25</sup>

Figure 1 illustrates the broad spectral range of operation of these microlasers. It gathers the spectra collected on the 6 different samples described in Table I. It should be noticed that for each sample, the lasing operation is obtained for microdisk diameters ranging from 3 to 12  $\mu\text{m}$ ; the diameters in Figure 1 are chosen in order to exhibit the most contrasted combs of modes under CW excitation, far below threshold. The microdisks are excited with a 266 nm laser through a microscope objective, with a large gaussian spot size (FWHM 10–12  $\mu\text{m}$ ). The emission is collected from the side of the microdisks with a 5 cm lens, coupled to a multimode fiber, and analyzed with a 55 cm spectrometer. Lasing action requires a strong peak power for the

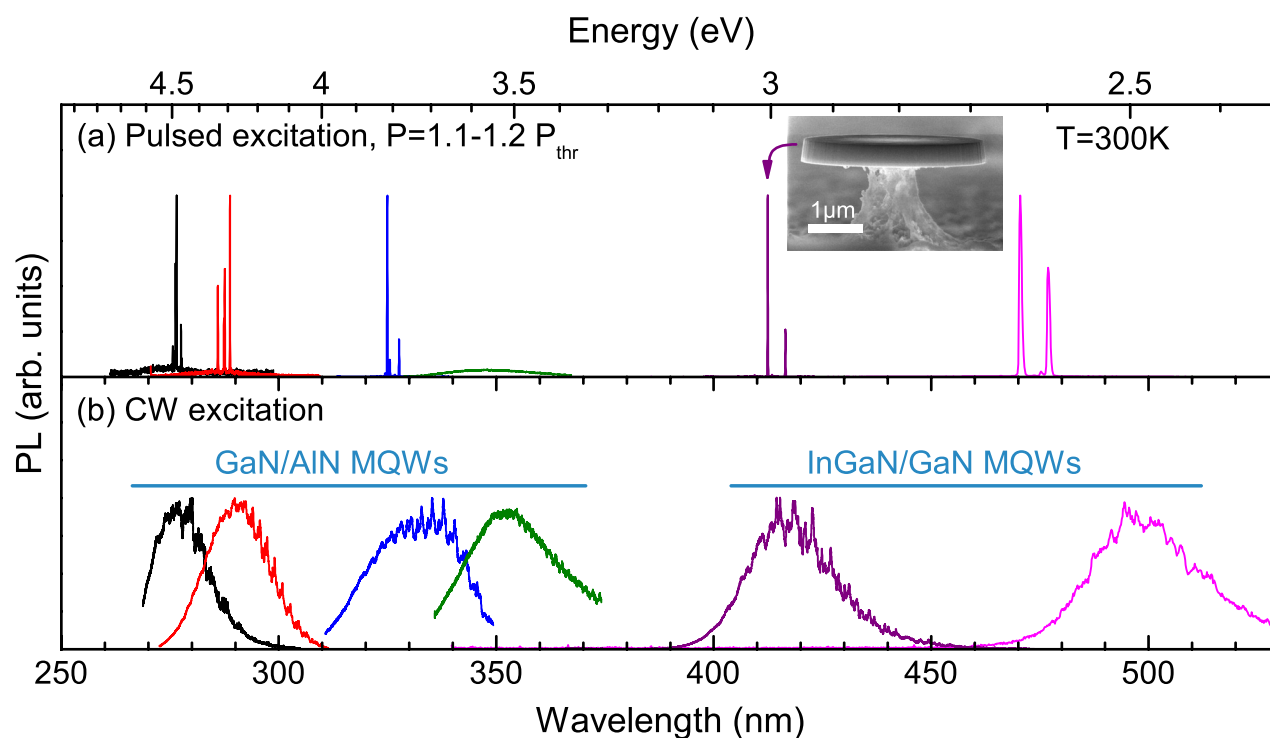


FIG. 1. Photoluminescence spectra of the 6 investigated microdisk samples (from left to right, GaN-1 to GaN-4, InGaN-1, InGaN-2); (a) microlaser spectrum above threshold, under pulsed optical pumping; (b) microdisk spectrum in the linear regime, under CW excitation. The inset presents the electron micrograph of a 4  $\mu\text{m}$  microdisk from the InGaN-1 series.

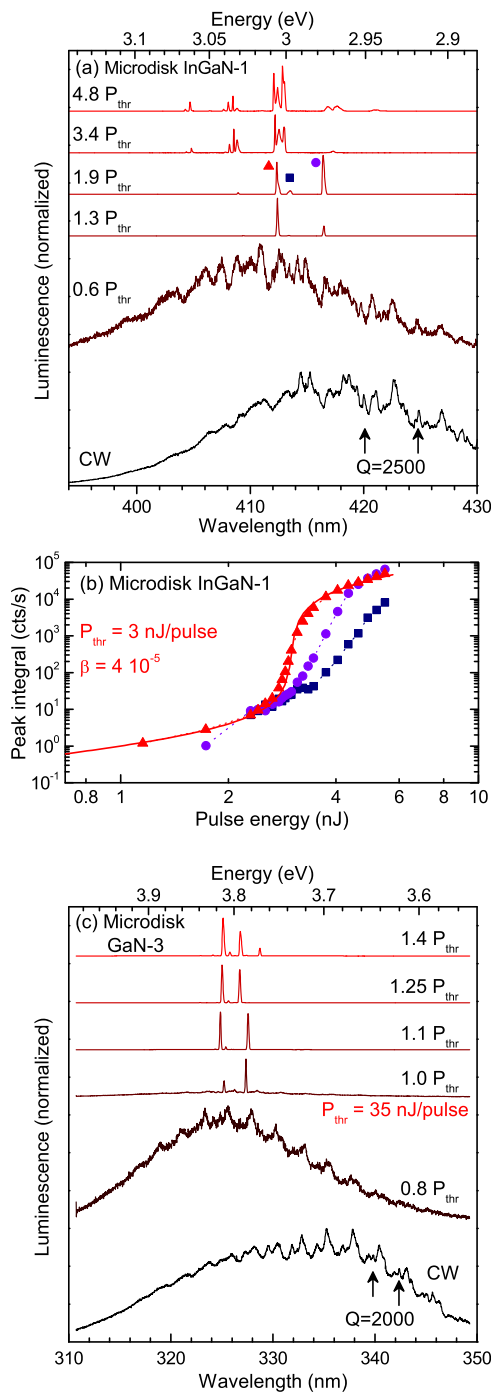


FIG. 2. (a) Photoluminescence spectra of a  $4\ \mu\text{m}$  microdisk in the sample InGaN-1, as a function of the pulsed laser excitation power; the CW spectrum of the same microdisk is presented for comparison. (b) Input-output characteristics of the 3 lasing modes marked on the panel (a); the symbols represent the peak integrals when the underlying  $15\ \text{nm}$ -broad background is subtracted; the plain red line shows the fit of the intensity of the first peak (triangles) by the microlaser rate equation model. (c) Photoluminescence spectra of a  $6\ \mu\text{m}$  microdisk in the sample GaN-3, as a function of the pulsed laser excitation power; the CW spectrum of the same microdisk is presented for comparison.

optical pumping, which is obtained through pulsed excitation ( $\lambda = 266\ \text{nm}$ ,  $400\ \text{ps}$  pulses at a repetition rate of  $4\ \text{kHz}$ ) with the same spot diameter. The lasing threshold  $P_{\text{thr}}$  is expressed in  $\text{mJ}\cdot\text{cm}^{-2}/\text{pulse}$  (Table I). It slightly varies from disk to disk for a given sample (typically 30%), but it is not correlated with the microdisk diameter within the investigated range of diameters, from  $3$  to  $12\ \mu\text{m}$ , as

discussed in Ref. 17. Investigating microdisks in this  $3$  to  $12\ \mu\text{m}$  range allows one to use an underetching that prevents significant modal absorption in the silicon pedestal.<sup>19</sup> We also varied the microdisk thickness without a visible impact on the lasing threshold. It appears that for the investigated range of microdisk quality factors ( $Q > 1000$ ), the microlaser threshold is mostly determined by the gain threshold of the active layer, as discussed later.

The detailed investigation of the microdisk laser operation is presented in Figures 2(a) and 2(b) for the microdisk InGaN-1, emitting at  $412\ \text{nm}$ . It is analyzed within the same framework as the microdisk GaN-1 in Ref. 17. The sharpest cavity modes observed under CW excitation reach a quality factor  $Q = 2500$ , representative of all microdisks (Table I). When the same microdisk is pumped with the pulsed excitation laser, the first lasing mode arises from a slightly broader mode. The strong peak power leads to a blueshift of  $30\ \text{meV}$  of the QW transition that is attributed both to the screening of the QW internal electric field and to the nascent band filling of the QW.<sup>26,27</sup> At  $P = 0.6 P_{\text{thr}}$ , this band filling bleaches the QW absorption on the high energy tail of the PL spectrum (between  $3$  and  $3.05\ \text{eV}$ ), so that some WGMs appear much more contrasted than on the CW spectrum: the QW absorption contribution to the WGM damping rate is suppressed at transparency. The onset of lasing is observed at  $3\ \text{eV}/412\ \text{nm}$ , and the gain band progressively extends to higher energies as the band filling increases. At the maximum pump power, the spectrum presents a well-defined structure of 5 groups of peak, corresponding to 5 consecutive values of the azimuthal eigennumber; the corresponding free spectral range ( $4.1\ \text{nm}$ ) is consistent with the microdisk modeling and our previous work.<sup>19</sup> The modes marked by a triangle and a circle correspond to the same radial and vertical indices and only differ by one azimuthal number. The input-output characteristics of the 3 marked lasing modes are presented in Figure 2(b). The intensity of the first lasing mode is analyzed through the standard rate equation model for microlasers (Annex in Ref. 17), and its emission coupling factor worth  $\beta = 4 \times 10^{-5}$ , limited by the multimode character of the microdisk resonator and possibly by the radiative efficiency of the active layer. The order of magnitude of  $\beta$  is comparable to the one of the  $3\ \mu\text{m}$  microdisk in the sample GaN-1.<sup>17</sup> Smaller microdisk diameters with a monomode vertical confinement would be required to approach single mode and large  $\beta$  threshold-less lasing, and a noticeable threshold reduction with the mode volume. The two next lasing modes follow a slower increase at threshold, which is attributed to the mode competition. Since the extraction of the  $\beta$  factor requires the clear observation of the lasing mode below the lasing threshold, it was not possible to measure it rigorously for larger microdisk diameters. For comparison, the spectra of a  $6\ \mu\text{m}$  microdisk from the sample GaN-3, emitting at  $330\ \text{nm}$ , are presented in Figure 2(c).

Table I presents the pumping threshold for each sample. We can observe a clear difference between the two families of QWs: the threshold is one order of magnitude smaller for InGaN/GaN QW microdisks ( $3\ \text{mJ}\cdot\text{cm}^{-2}$  per pulse) than for GaN/AlN QW microdisks ( $\sim 30\ \text{mJ}\cdot\text{cm}^{-2}$ ). This can be interpreted as the difference between resonant and non-resonant excitation. Indeed, the laser energy is

below the AlN bandgap and above the GaN bandgap. The 266 nm laser pumps the excited states of the GaN/AlN QW, and the 10 QWs can only absorb part of it. On the contrary, the entire pulse energy is absorbed by the GaN barrier in the case of InGaN QWs, leading to a larger carrier density per QW if we assume that all carriers are transferred from the barrier to the well.

This study of the entire series of active layers underlines the interest of the microdisk geometry in order to validate the gain potentialities of the investigated active layers, since such a comparison would have been much more difficult to obtain from a series of photonic crystal microlasers. For example, we could not reach lasing on a sample similar to the InGaN-1 microlaser, for which the density of pit defects ( $10^9 \text{ cm}^{-2}$ ) was 10 times larger than for the other samples ( $10^7$ – $10^8 \text{ cm}^{-2}$ ); this confirms that the control of the density of defects in the buffer and active layers is one of the key features enabling the laser operation. Concerning the series of GaN/AlN microlasers, we observe that the microlaser series GaN-4, embedding the thickest GaN/AlN QWs, cannot be brought to lasing action within the investigated range of pump energies, despite a defect density comparable to the samples GaN-1,2,3; this is qualitatively attributed to the weaker oscillator strength/weaker gain of these QWs due to the onset of the QCSE.

We should emphasize the original choice of QW design of the UV emitting samples: GaN/AlGaIn QWs or AlGaIn/AlGaIn QWs are usually chosen for UV-emitting ridge lasers (see Ref. 28 for a review), in order to limit the detrimental effect of the QCSE on the QW oscillator strength; such active layers require the use of very thick and complex buffer layers in order to reduce the defect density and improve the QW radiative efficiency. Here, we demonstrate that the use of binary materials (GaN and AlN) for the well and the barrier provides a powerful alternative: there is no contribution of the alloy disorder to the spectral broadening of the emission, and the small interface roughness limits the impact of monolayer fluctuations on the QW transition energy. Moreover, the use of very thin QWs limits the role of the QCSE for the microlaser series GaN-1 to GaN-3, as confirmed by the limited blueshift of the emission at the lasing threshold; therefore, the QWs provide gain up to 330 nm. The situation is slightly different in the case of the InGaIn-2 QW microlaser: we observe a blueshift of 30 nm/160 meV for the sample InGaIn-2 that we attribute to the combined effects of the screening of the QCSE and of the carrier localization since a ternary alloy is used for the quantum well layer.

The present GaN-on-silicon platform compares well with other recent approaches. The measured threshold pump energy of the InGaIn/GaN QW microlasers is a factor 5–10 larger than the one reported for microdisk lasers embedding InGaIn/GaN QDs,<sup>13</sup> fractional quantum wells,<sup>12</sup> or MQWs<sup>10</sup> under pulsed excitation. It can hardly be compared to the two demonstrated CW operated microdisk lasers, emitting in the blue<sup>8</sup> and in the green<sup>15</sup> spectral ranges with structures grown on sapphire or grown by metalorganic chemical vapour deposition (MOCVD). Most of the other microlaser demonstrations, including those in the UV spectral range, were performed at cryogenic temperatures;<sup>14,16,29</sup> this

usually leads to a strong reduction of the threshold, thus confirming that the emission efficiency of the active layer is the main parameter determining the microlaser threshold. This underlines the importance of the reduction of the defect density in the underlying buffer layers: the achieved dislocation density of typically  $10^{10} \text{ cm}^{-2}$  is low enough so that non-radiative recombinations are not taking over gain at large carrier densities, as recently investigated in AlGaIn QWs.<sup>30</sup>

To conclude, we have demonstrated the large spectral tunability of nitride-on-silicon MQWs for UV to visible microlasers, over a 200 nm spectral range. The comparison of different active layers and microdisk diameters allows us to evidence the respective roles of the resonant or non-resonant character of the optical excitation, of the defect density and the related room-temperature emission efficiency, and the QCSE. The broad tunability paves the way to the development of a UV-visible integrated photonic platform embedding microlasers, possibly addressing multiple wavelengths. A further step will deal with the electrical injection, following the recent progresses in electrically injected InGaIn lasers on Si-substrates.<sup>31</sup>

The authors acknowledge support from the projects GANEX (ANR-11-LABX-0014) and QUANONIC (ANR-13-BS10-0010). GANEX belongs to the public funded “Investissements d’Avenir” program managed by the French ANR agency. This work was also partly supported by the RENATECH network.

<sup>1</sup>B. Thubthimthong, T. Sasaki, and K. Hane, “Asymmetrically and vertically coupled hybrid Si/GaN microring resonators for on-chip optical interconnects,” *IEEE Photonics J.* **7**, 1–11 (2015).

<sup>2</sup>Y. Wang, G. Zhu, W. Cai, X. Gao, Y. Yang, J. Yuan, Z. Shi, and H. Zhu, “On-chip photonic system using suspended p-n junction InGaIn/GaN multiple quantum wells device and multiple waveguides,” *Appl. Phys. Lett.* **108**, 162102 (2016).

<sup>3</sup>Y.-D. Yang, Y. Zhang, Y.-Z. Huang, and A. W. Poon, “Direct-modulated waveguide-coupled microspiral disk lasers with spatially selective injection for on-chip optical interconnects,” *Opt. Express* **22**, 824 (2014).

<sup>4</sup>S. Chang, N. B. Rex, R. K. Chang, G. Chong, and L. J. Guido, “Stimulated emission and lasing in whispering-gallery modes of GaN microdisk cavities,” *Appl Phys Lett.* **75**, 166–168 (1999).

<sup>5</sup>H. W. Choi, K. N. Hui, P. T. Lai, P. Chen, X. H. Zhang, S. Tripathy, J. H. Teng, and S. J. Chua, “Lasing in GaN microdisks pivoted on Si,” *Appl. Phys. Lett.* **89**, 211101 (2006).

<sup>6</sup>S. W. Chen, T. C. Lu, Y. J. Hou, T. C. Liu, H. C. Kuo, and S. C. Wang, “Lasing characteristics at different band edges in GaN photonic crystal surface emitting lasers,” *Appl. Phys. Lett.* **96**, 071108 (2010).

<sup>7</sup>R. Chen, H. D. Sun, T. Wang, K. N. Hui, and H. W. Choi, “Optically pumped ultraviolet lasing from nitride nanopillars at room temperature,” *Appl Phys Lett.* **96**, 241101 (2010).

<sup>8</sup>A. C. Tamboli, E. D. Haberer, R. Sharma, K. H. Lee, S. Nakamura, and E. L. Hu, “Room-temperature continuous-wave lasing in GaN/InGaIn microdisks,” *Nat. Photonics* **1**, 61–64 (2007).

<sup>9</sup>D. Simeonov, E. Feltrin, H.-J. Buhlmann, T. Zhu, A. Castiglia, M. Mosca, J.-F. Carlin, R. Butté, and N. Grandjean, “Blue lasing at room temperature in high quality factor GaN/AlInN microdisks with InGaIn quantum wells,” *Appl. Phys. Lett.* **90**, 061106 (2007).

<sup>10</sup>G. D. Chern, H. E. Tureci, A. D. Stone, R. K. Chang, M. Kneissl, and N. M. Johnson, “Unidirectional lasing from InGaIn multiple-quantum-well spiral-shaped micropillars,” *Appl. Phys. Lett.* **83**, 1710–1712 (2003).

<sup>11</sup>N. V. Triviño, R. Butté, J.-F. Carlin, and N. Grandjean, “Continuous wave blue lasing in III-nitride nanobeam cavity on silicon,” *Nano Lett.* **15**, 1259–1263 (2015).

<sup>12</sup>N. Niu, A. Woolf, D. Wang, T. Zhu, Q. Quan, R. A. Oliver, and E. L. Hu, “Ultra-low threshold gallium nitride photonic crystal nanobeam laser,” *Appl. Phys. Lett.* **106**, 231104 (2015).

- <sup>13</sup>I. Aharonovich, A. Woolf, K. J. Russell, T. Zhu, N. Niu, M. J. Kappers, R. A. Oliver, and E. L. Hu, "Low threshold, room-temperature microdisk lasers in the blue spectral range," *Appl. Phys. Lett.* **103**, 021112 (2013).
- <sup>14</sup>A. Woolf, T. Puchtler, I. Aharonovich, T. Zhu, N. Niu, D. Wang, R. Oliver, and E. L. Hu, "Distinctive signature of indium gallium nitride quantum dot lasing in microdisk cavities," *Proc. Natl. Acad. Sci.* **111**, 14042 (2014).
- <sup>15</sup>M. Athanasiou, R. Smith, B. Liu, and T. Wang, "Room temperature continuous-wave green lasing from an InGaN microdisk on silicon," *Sci. Rep.* **4**, 7250 (2014).
- <sup>16</sup>M. Bürger, G. Callsen, T. Kure, A. Hoffmann, A. Pawlis, D. Reuter, and D. J. As, "Lasing properties of non-polar GaN quantum dots in cubic aluminum nitride microdisk cavities," *Appl. Phys. Lett.* **103**, 021107 (2013).
- <sup>17</sup>J. Sellés, C. Brimont, G. Cassabois, P. Valvin, T. Guillet, I. Roland, Y. Zeng, X. Checoury, P. Boucaud, M. Mexis, F. Semond, and B. Gayral, "Deep-UV nitride-on-silicon microdisk lasers," *Sci. Rep.* **6**, 21650 (2016).
- <sup>18</sup>S. Islam, V. Protasenko, S. Rouvimov, H. (Grace) Xing, and D. Jena, "Sub-230 nm deep-UV emission from GaN quantum disks in AlN grown by a modified Stranski-Krastanov mode," *Jpn. J. Appl. Phys.* **55**, 05FF06 (2016).
- <sup>19</sup>M. Mexis, S. Sergent, T. Guillet, C. Brimont, T. Bretagnon, B. Gil, F. Semond, M. Leroux, D. Néel, S. David, X. Chécoury, and P. Boucaud, "High quality factor nitride-based optical cavities: microdisks with embedded GaN/Al(GaN) quantum dots," *Opt. Lett.* **36**, 2203–2205 (2011).
- <sup>20</sup>D. Néel, S. Sergent, M. Mexis, D. Sam-Giao, T. Guillet, C. Brimont, T. Bretagnon, F. Semond, B. Gayral, S. David, X. Checoury, and P. Boucaud, "AlN photonic crystal nanocavities realized by epitaxial conformal growth on nanopatterned silicon substrate," *Appl. Phys. Lett.* **98**, 261106 (2011).
- <sup>21</sup>D. Sam-Giao, D. Néel, S. Sergent, B. Gayral, M. J. Rashid, F. Semond, J. Y. Duboz, M. Mexis, T. Guillet, C. Brimont, S. David, X. Checoury, and P. Boucaud, "High quality factor AlN nanocavities embedded in a photonic crystal waveguide," *Appl. Phys. Lett.* **100**, 191104 (2012).
- <sup>22</sup>C. Brimont, T. Guillet, S. Rousset, D. Néel, X. Checoury, S. David, P. Boucaud, D. Sam-Giao, B. Gayral, M. J. Rashid, and F. Semond, "Imaging of photonic modes in an AlN-based photonic crystal probed by an ultra-violet internal light source," *Opt. Lett.* **38**, 5059–5062 (2013).
- <sup>23</sup>I. Roland, Y. Zeng, Z. Han, X. Checoury, C. Blin, M. El Kurdi, A. Ghrib, S. Sauvage, B. Gayral, C. Brimont, T. Guillet, F. Semond, and P. Boucaud, "Near-infrared gallium nitride two-dimensional photonic crystal platform on silicon," *Appl. Phys. Lett.* **105**, 011104 (2014).
- <sup>24</sup>Y. Zeng, I. Roland, X. Checoury, Z. Han, M. El Kurdi, S. Sauvage, B. Gayral, C. Brimont, T. Guillet, M. Mexis, F. Semond, and P. Boucaud, "Resonant second harmonic generation in a gallium nitride two-dimensional photonic crystal on silicon," *Appl. Phys. Lett.* **106**, 081105 (2015).
- <sup>25</sup>Y. Zeng, I. Roland, X. Checoury, Z. Han, M. El Kurdi, S. Sauvage, B. Gayral, C. Brimont, T. Guillet, F. Semond, and P. Boucaud, "Imaging of photonic crystal localized modes through third-harmonic generation," *ACS Photonics* **3**, 1240 (2016).
- <sup>26</sup>S. Kalliakos, P. Lefebvre, and T. Taliercio, "Nonlinear behavior of photo-absorption in hexagonal nitride quantum wells due to free carrier screening of the internal fields," *Phys. Rev. B.* **67**, 205307 (2003).
- <sup>27</sup>T. Bretagnon, S. Kalliakos, P. Lefebvre, P. Valvin, B. Gil, N. Grandjean, A. Dussaigne, B. Damilano, and J. Massies, "Time dependence of the photoluminescence of GaN/AlN quantum dots under high photoexcitation," *Phys. Rev. B.* **68**, 205301 (2003).
- <sup>28</sup>V. N. Jmerik, E. V. Lutsenko, and S. V. Ivanov, "Plasma-assisted molecular beam epitaxy of AlGaIn heterostructures for deep-ultraviolet optically pumped lasers," *Phys. Status Solidi A* **210**, 439–450 (2013).
- <sup>29</sup>E. D. Haberer, R. Sharma, C. Meier, A. R. Stonas, S. Nakamura, S. P. DenBaars, and E. L. Hu, "Free-standing, optically pumped, GaN/InGaN microdisk lasers fabricated by photoelectrochemical etching," *Appl. Phys. Lett.* **85**, 5179–5181 (2004).
- <sup>30</sup>K. Ban, J. Yamamoto, K. Takeda, K. Ide, M. Iwaya, T. Takeuchi, S. Kamiyama, I. Akasaki, and H. Amano, "Internal quantum efficiency of whole-composition-range AlGaIn multiquantum wells," *Appl. Phys. Express* **4**, 052101 (2011).
- <sup>31</sup>Y. Sun, K. Zhou, Q. Sun, J. Liu, M. Feng, Z. Li, Y. Zhou, L. Zhang, D. Li, S. Zhang, M. Ikeda, S. Liu, and H. Yang, "Room-temperature continuous-wave electrically injected InGaN-based laser directly grown on Si," *Nat. Photonics* **10**, 595 (2016).